Electronic structure of Ag_xPt_{1-x} alloys

H. Ebert
Institut für Physikalische Chemie der Universität München, Sophienstrasse 11, D-8000 München 2, Federal Republic of Germany

P. Weinberger
Institut für Technische Elektrochemie, Technische Universität Wien, Getreidemarkt 9, A-1060 Wien, Austria

J. Voitländer
Institut für Physikalische Chemie der Universität München, Sophienstrasse 11, D-8000 München 2, Federal Republic of Germany

(Received 15 October 1984)

Fully relativistic Korringa-Kohn-Rostoker coherent-potential approximation calculations are performed for Ag_xPt_{1-x}, $x=0.06$, 0.15, 0.30, 0.40, 0.50, 0.70, and 0.90. The electronic structure of the Ag_xPt_{1-x} alloys is discussed in terms of densities of states, $d^{3/2}$-like and $d^{5/2}$-like partial local densities of states for the components Ag and Pt, and in terms of Bloch spectral functions. For all alloys "Fermi-surface cuts" in the ΓXK, ΓXU, and ΓKU planes are shown. The variation of the unenhanced density of states at the Fermi energy with the concentration x agrees rather well with the variation of the experimental molar susceptibilities. From the Bloch spectral functions, but also, from the densities of states, it is found that the electronic structure undergoes strong changes when the molar fraction varies.

I. INTRODUCTION

The Korringa-Kohn-Rostoker coherent potential approximation[1-3] (KKR-CPA) proved to be a very reliable method of describing the electronic structure of substitutionally disordered alloys. Since this method can be formulated fully relativistically,[4] alloys containing heavy elements can also be investigated. The Ag_xPt_{1-x} system is interesting for a number of reasons: experimentally, since a large amount of data is available, and theoretically because it is the first alloy system containing a $4d$ and a $5d$ element to be described in terms of the KKR-CPA method. Previous KKR-CPA calculations dealt with elements of the same row such as Cu_xNi_{1-x} (see Refs. 1 and 2), Ag_xPd_{1-x},[5] or Au_xPt_{1-x},[6] or with alloy systems containing $3d$ and $4d$ elements such as Cu_xPd_{1-x},[7] or $3d$ and $5d$ elements such as Ni_xPt_{1-x}.[8] Since for Pt relativistic effects are of crucial importance, and since also for Ag these effects are not negligible, the use of the fully relativistic KKR-CPA method is an absolute necessity.

Experimentally, the ultraviolet photoemission spectra (UPS) for Ag-rich Ag_xPt_{1-x} alloys are particularly interesting, since they show a kind of two-peak structure in the region of the Ag sp band which is not observed in the Ag_xPd_{1-x} system. The rapid decay of the molar susceptibility for Pt-rich Ag_xPt_{1-x} alloys with increasing Ag concentration is another piece of experimental data deserving theoretical investigation. As far as nuclear-spin-lattice relaxation rates for Ag and Pt are concerned, a separate paper[9] provides a fully relativistic formulation of these quantities and uses the present results for a calculation of $(T_1T)^{-1}$ rates in Ag_xPt_{1-x}.

II. NUMERICAL ASPECTS

The fully relativistic KKR-CPA method[4] is used to calculate the site-diagonal scattering-path operator and the effective scattering amplitudes. The scattering potentials are constructed non-self-consistently by the so-called Mattheiss prescription in the same way as described by Staunton *et al.*[8] The lattice parameters[10] applied for the Ag_xPt_{1-x} system are shown in Fig. 1 as a function of the Ag concentration. The density of states, component densities of states, and the angular-momentum-dependent densities of states for the components are calculated ac-

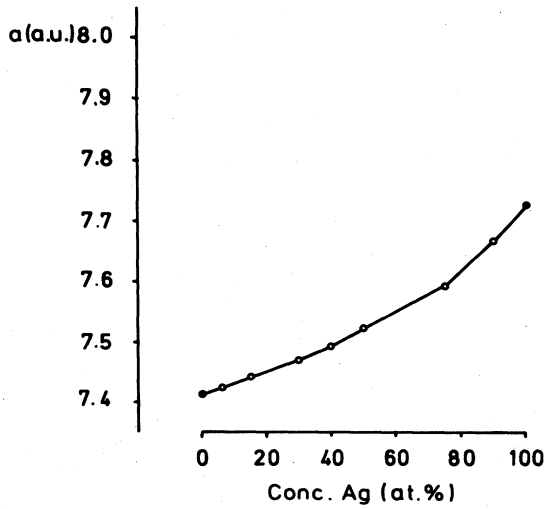

FIG. 1. Lattice constants for Ag_xPt_{1-x} (a.u.) (Ref. 10).

cording to Ref. 4. For the k- and energy-dependent Bloch spectral functions the formulas given in Appendix 1 of Ref. 6 are used. For the Ag-rich alloys it was difficult to obtain convergence concerning the CPA condition[4] in the middle of the conduction band. These problems could be circumvented by the use of complex energies, for which convergence could easily be achieved. The effective scattering amplitudes and the site-diagonal scattering-path operator for real energies were then determined by analytical continuation to the real-energy axis by means of the Cauchy-Riemann conditions.

III. RESULTS

Figures 2(a) and 2(b) show the band structure along [100] for the case that in $Ag_{70}Pt_{30}$ all sites would be occupied by either (a) Ag or (b) Pt, i.e., they show band structures along Γ—X for Ag and Pt corresponding to the lattice constant in $Ag_{70}Pt_{30}$. As one can see from these figures, the d-band width of Ag (top X_7^+—bottom X_7^+: 0.266 Ry) is considerably smaller than that in Pt (0.469 Ry). Most of the Ag d bands are in the regime of the Pt $d^{3/2}$ band and do show considerable splitting due to relativistic effects. It is interesting to note that at X the total bandwidth ($X_6^- - X_6^+$) is about the same for both cases, namely 0.676 and 0.658 Ry for Ag and Pt, respectively.

In Figs. 3(a) and 3(b) the d-like effective scattering amplitudes are shown for Ag_6Pt_{94} and $Ag_{90}Pt_{10}$. These two figures are particularly interesting since they show that even for small concentrations the scattering in the d channels is remarkably inelastic. At the Pt-rich end, for Ag_6Pt_{94}, the structures for the $d^{5/2}$ channels indicate a split-$d^{5/2}$-band behavior. At the Ag-rich end, for $Ag_{90}Pt_{10}$, the $d^{3/2}$ channel still shows considerable absorption.

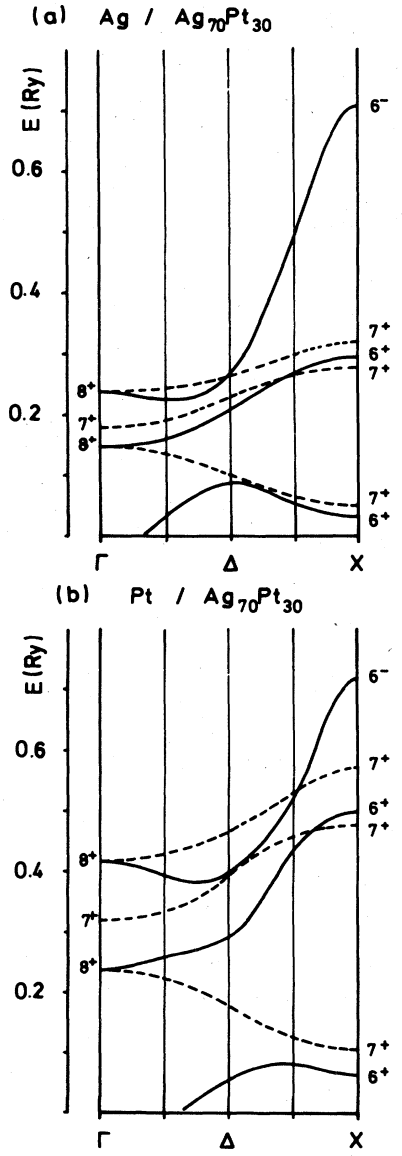

FIG. 2. Band structure along [100] for (a) Ag and (b) Pt in $Ag_{70}Pt_{30}$. Solid lines indicate bands of Δ_6 symmetry and dashed lines those of Δ_7 symmetry.

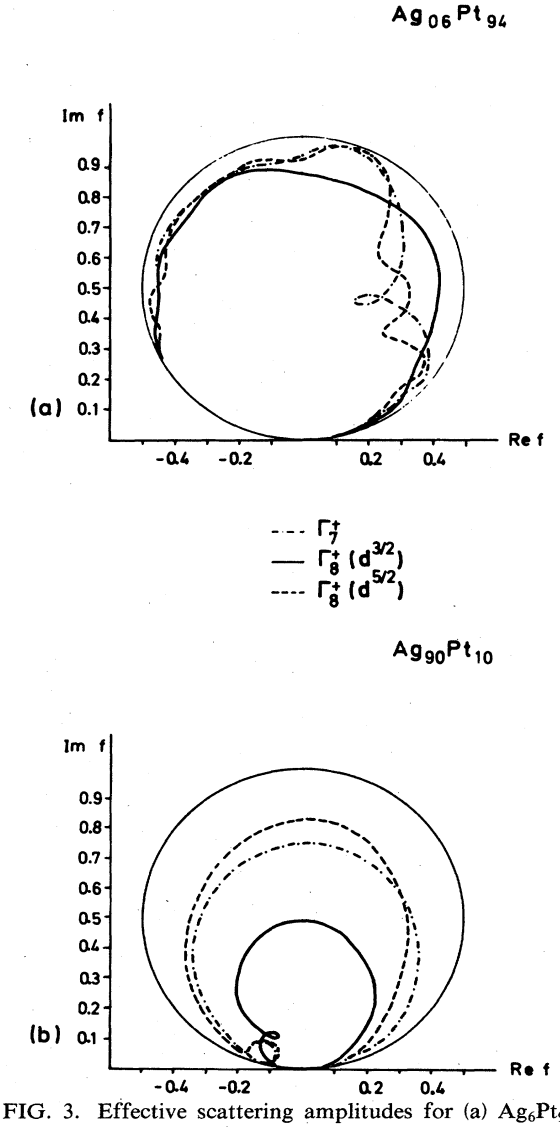

FIG. 3. Effective scattering amplitudes for (a) Ag_6Pt_{94} and (b) $Ag_{90}Pt_{10}$

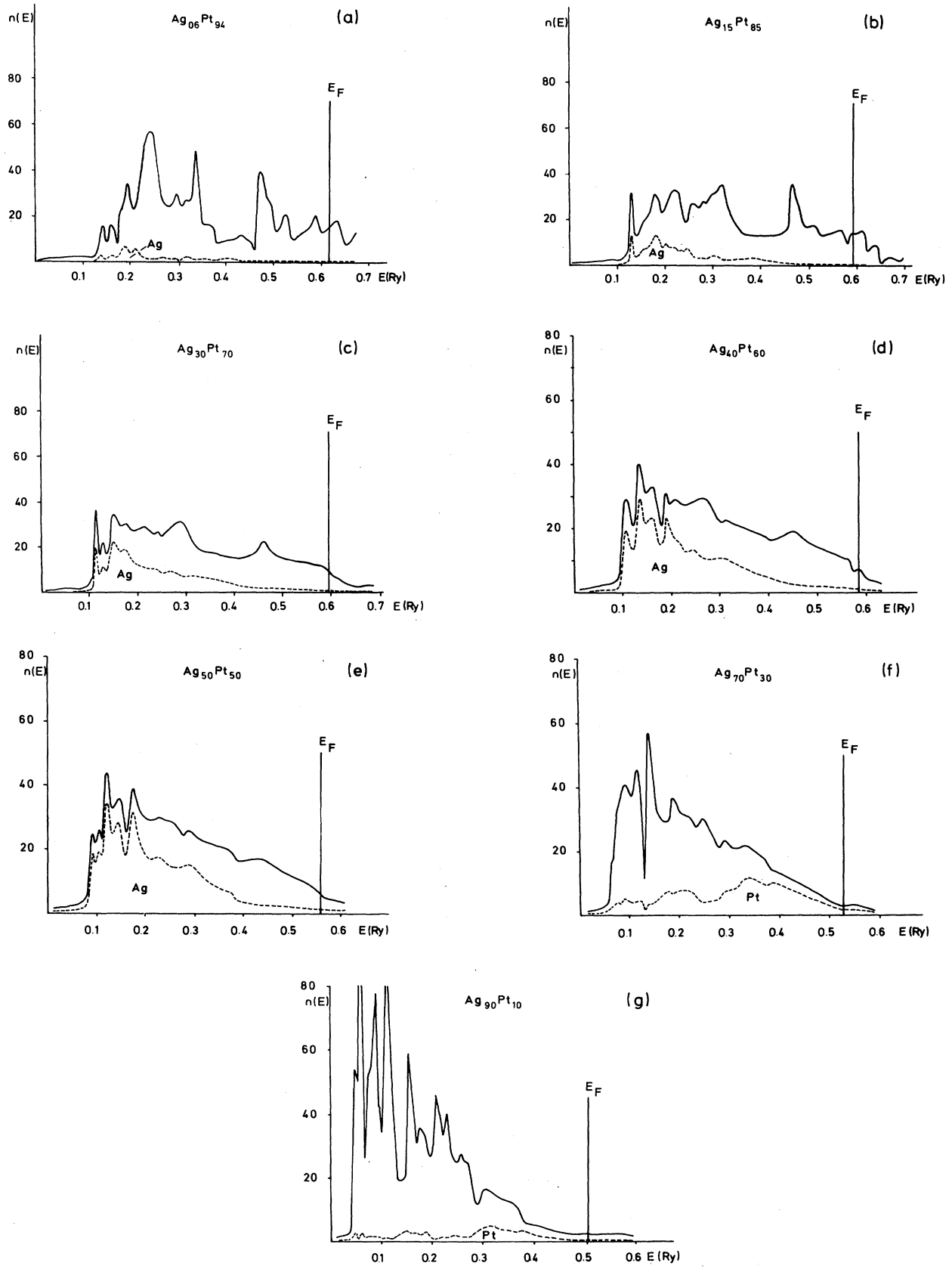

FIG. 4. Density of states for (a) Ag_6Pt_{94}, (b) $Ag_{15}Pt_{85}$, (c) $Ag_{30}Pt_{70}$, (d) $Ag_{40}Pt_{60}$, (e) $Ag_{50}Pt_{50}$, (f) $Ag_{70}Pt_{30}$, and (g) $Ag_{90}Pt_{10}$. The contribution of one of the components to the density of states is shown by a dashed line.

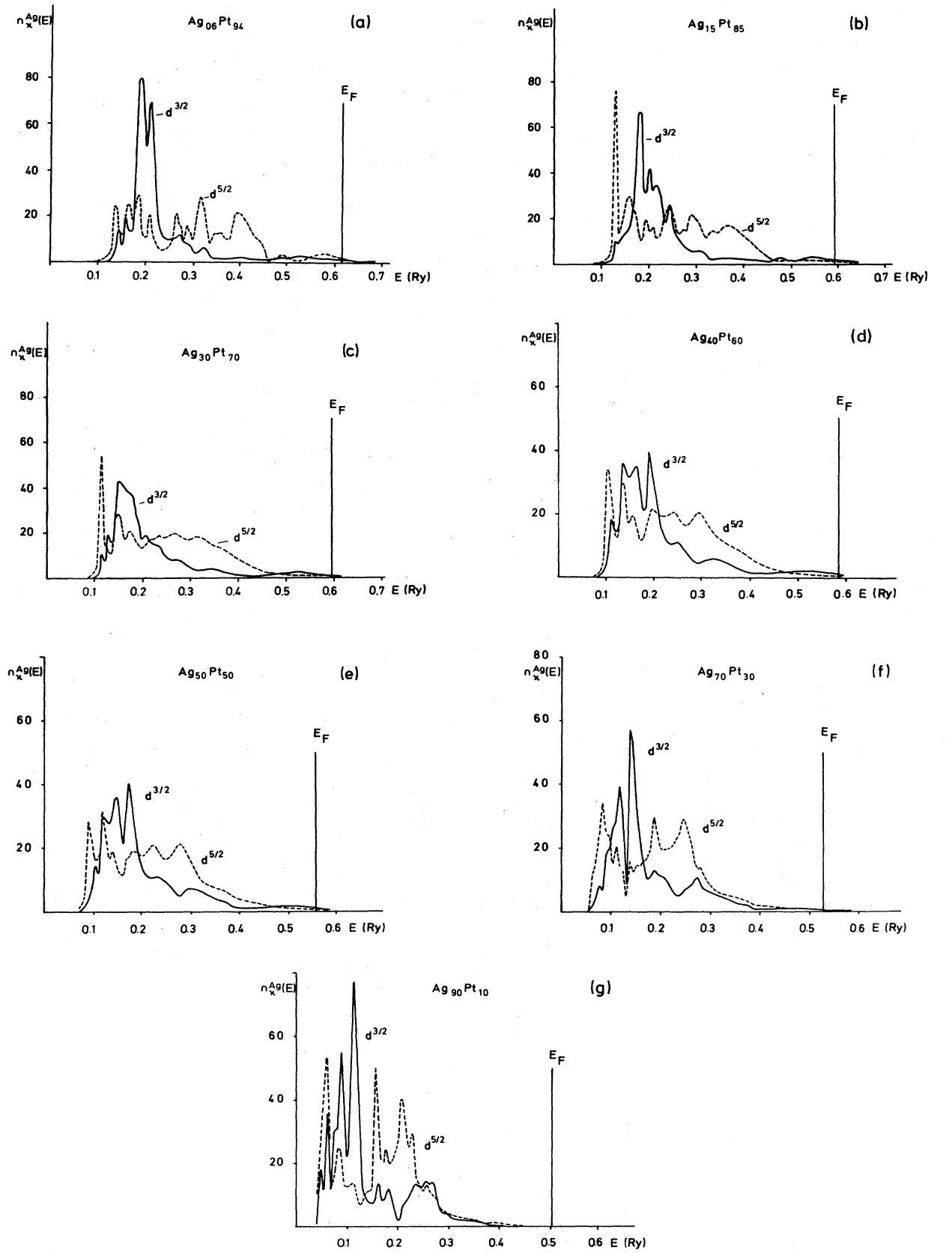

FIG. 5. $d^{3/2}$-like (solid line) and $d^{5/2}$-like (dashed line) partial local densities of states of Ag for (a) Ag_6Pt_{94}, (b) $Ag_{15}Pt_{85}$, (c) $Ag_{30}Pt_{70}$, (d) $Ag_{40}Pt_{60}$, (e) $Ag_{50}Pt_{50}$, (f) $Ag_{70}Pt_{30}$, and (g) $Ag_{90}Pt_{10}$.

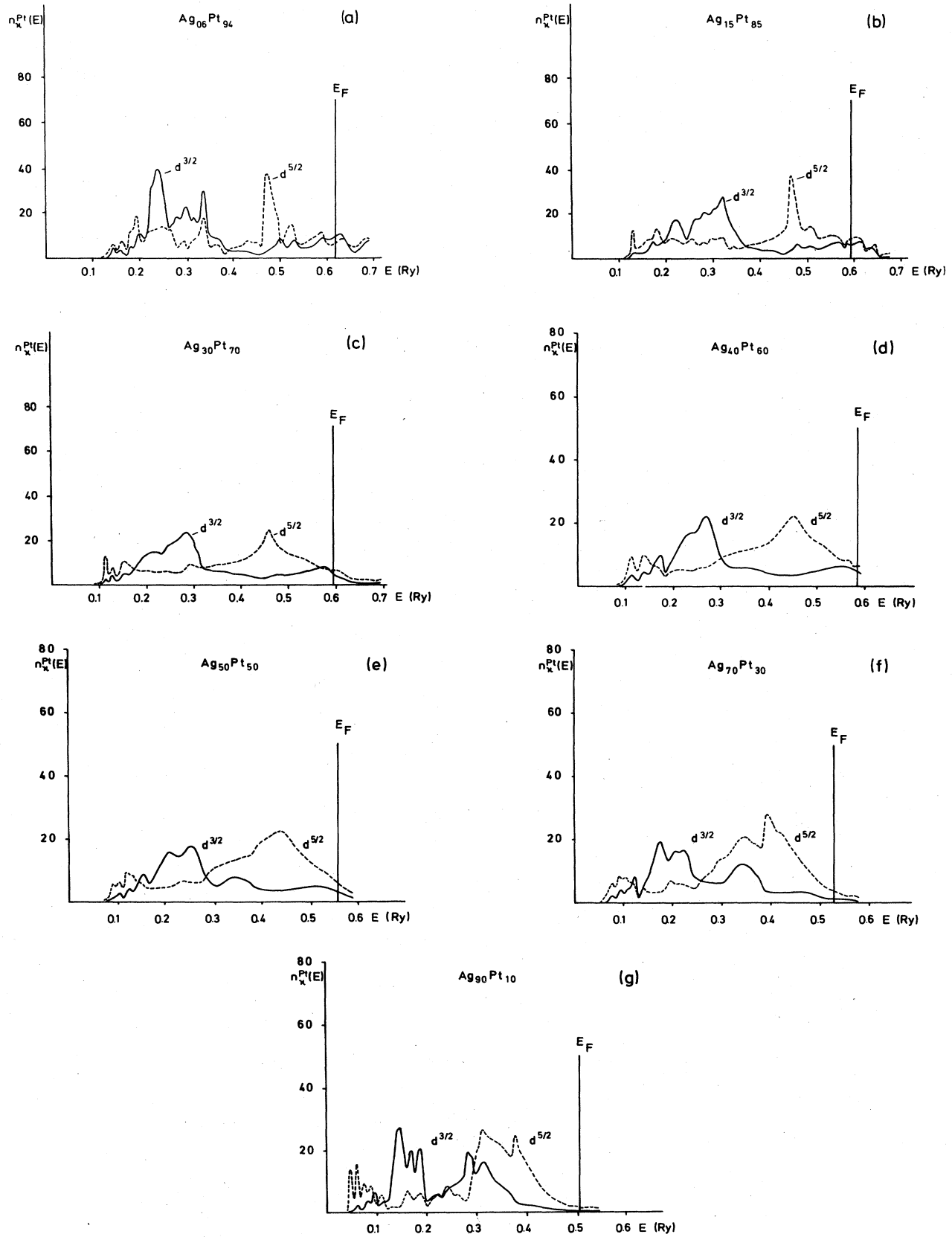

FIG. 6. $d^{3/2}$-like (solid line) and $d^{5/2}$-like partial local densities of states of Pt for (a) Ag_6Pt_{94}, (b) $Ag_{15}Pt_{85}$, (c) $Ag_{30}Pt_{70}$, (d) $Ag_{40}Pt_{60}$, (e) $Ag_{50}Pt_{50}$, (f) $Ag_{70}Pt_{30}$, and (g) $Ag_{90}Pt_{10}$.

The density of states for all the investigated Ag_xPt_{1-x} alloys is displayed in Fig. 4, together with the component density of states for Ag, weighted by the molar fraction for $x \leq 0.5$, and together with the corresponding quantity for Pt for $x > 0.5$. With increasing Ag concentration one can see that (a) Ag (impuritylike) peaks are built up at the bottom of the Pt $d^{3/2}$—like bands, and (b) that the structure in the regime of the Pt $d^{5/2}$—like bands, particularly in the vicinity of the Fermi energy, is flattened out. For Ag-rich alloys the peaks at the beginning of the valence band are already very much like those in pure Ag; however, at about 0.15—0.20 Ry below the Fermi energy, remainders of the Pt $d^{5/2}$ band can be seen.

The partial local $d^{3/2}$- and $d^{5/2}$-like densities of states for Ag and Pt are displayed in Figs. 5 and 6, respectively. In the series for Ag one can see sharp peaks arising at the bottom of the Pt $d^{3/2}$ band. These peaks shift with increasing Ag concentration toward lower energies, while concomitantly the peak in the $d^{5/2}$-like density of states at about 0.4 Ry is dying out from $x=0.06$ to 0.3, to be rebuilt up for higher concentrations of Ag at lower energies. In the series of d-like partial local densities of states for Pt, one can see that the structure in both the $d^{3/2}$-like and $d^{5/2}$-like partial local densities of states vanishes very quickly with increasing Ag concentration. For $Ag_{90}Pt_{10}$, a region of "backscattering" at energies less than about 0.25 Ry seems to be separated from a region comprised by a two-peak structure in the $d^{3/2}$ as well as the $d^{5/2}$ partial local density of states. It should be noted that all partial local densities of states refer to the angular-momentum decomposition of the "muffin-tin" density of states[4] and are therefore not weighted by the molar fraction x.

In Fig. 7 the unenhanced density of states at the Fermi energy (theoretical linear coefficient of the specific heat, γ) is plotted versus the Ag concentration, together with the experimental molar susceptibility.[11] Also shown in this figure are the theoretical values of γ for the pure metals Pt (Ref. 12) and Ag (Ref. 13). The theoretical γ values in Fig. 7 reproduce rather well the sharp decrease in the experimental molar susceptibility at the Pt-rich end. The reason for this sharp decay of the linear coefficient of the specific heat can be seen either from Fig. 4 or Fig. 8, containing "Fermi-surface" cuts in the ΓXK, ΓXU, and ΓKU planes.

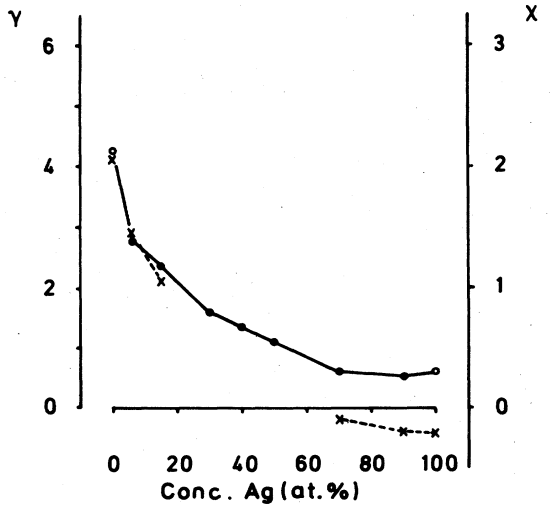

FIG. 7. Theoretical values (solid circles, solid line) for the linear coefficient γ (cal/mol^{-1}K^{-2}). Open circles are the theoretical γ values for pure Pt (Ref. 12) and Ag (Ref. 13). The crosses (dashed line) correspond to the experimental values (Ref. 11) for the molar susceptibility (10^{-4} cm^{-3} mol^{-1}).

In Fig. 8 Bloch spectral functions along a set of k rays at the Fermi energy are displayed in terms of the position of peaks and their half-width in momentum space. If the half-width in momentum space is small compared to the scale of the Brillouin zone, an alloy is said to have a well-defined Fermi surface. This is definitely the case for $Ag_{90}Pt_{10}$ and $Ag_{70}Pt_{30}$. For $Ag_{90}Pt_{10}$ the half-width coincides with the line shown. Because of Ag impuritylike states at the bottom of the Pt d bands, the Fermi energy in Ag_6Pt_{94} is lowered with respect to pure Pt. However, here one can already see parts of the well-known Fermi surface for pure Pt, namely the first Γ-centered sheet and the second sheet in the ΓXK plane. For pure Pt along Γ—K the second band vanishes, leaving a kind of fin in the ΓXU and ΓKU planes. One can clearly see this fin evolving, looking, in turn, at Figs. 8(c), 8(b), and finally 8(a). The considerable half-width—even for small concentrations of Ag—is one of the reasons for the sharp decay in γ for Pt-rich alloys. For Ag-rich alloys, Figs. 8(f) and 8(g) show the building up of the well-known neck of the Fermi surface for pure Ag.

In Fig. 9 the Bloch spectral functions at $\mathbf{k}=(0,0,0)$ are shown as functions of the energy parameter E. In Fig. 9(a) the three peaks essentially comprise the Pt Γ_8^+ ($d^{3/2}$), Γ_7^+, and Γ_8^+ ($d^{5/2}$) states. It is interesting to note that the Γ_7^+-like and Γ_8^+ ($d^{5/2}$)—like peaks are drastically decreased in intensity by going from $x=0.15$ to 0.30, and that also the separation in energy for these two peaks is decreased. At $x=0.5$ only one rather broad peak is a remainder from the Pt $d^{5/2}$—like states at Γ. This remaining peak is further decreased with increasing Ag concentration and is shifted towards lower energies. For $Ag_{90}Pt_{10}$ one can see the well-defined Γ_7^+ and Γ_8^+-like peaks for Ag and a leftover from the Pt states.

Figure 10, finally, represents an attempt to follow the peak positions in the Bloch spectral functions at $\mathbf{k}=(0,0,0)$ as a function of the concentration. In this figure one can see the complexity of changes in the electronic structure going from Pt-rich to Ag-rich alloys. While the Γ_7^+ and the top Γ_8^+ states for Pt die out with increasing Ag concentration, the lower Pt Γ_8^+ ($d^{3/2}$)—like state seems to get absorbed in the Ag $d^{5/2}$ states around $x=0.4$. This particular feature of the Bloch spectral functions partly explains the relative structurelessness of the density of states for $0.3 \leq x \leq 0.7$. It should be noted, however, that in Fig. 10 decisive assignment of peaks can be given only for well-defined peaks, such as, for example, the sharp Ag-like states in $Ag_{90}Pt_{10}$.

IV. DISCUSSION

Ag-rich alloys ($Ag_{98}Pt_2$ and $Ag_{90}Pt_{10}$) were investigated experimentally in terms of UPS spectra.[14,15] For $Ag_{98}Pt_2$, a two-peak structure is observed[14] in the region of the Ag

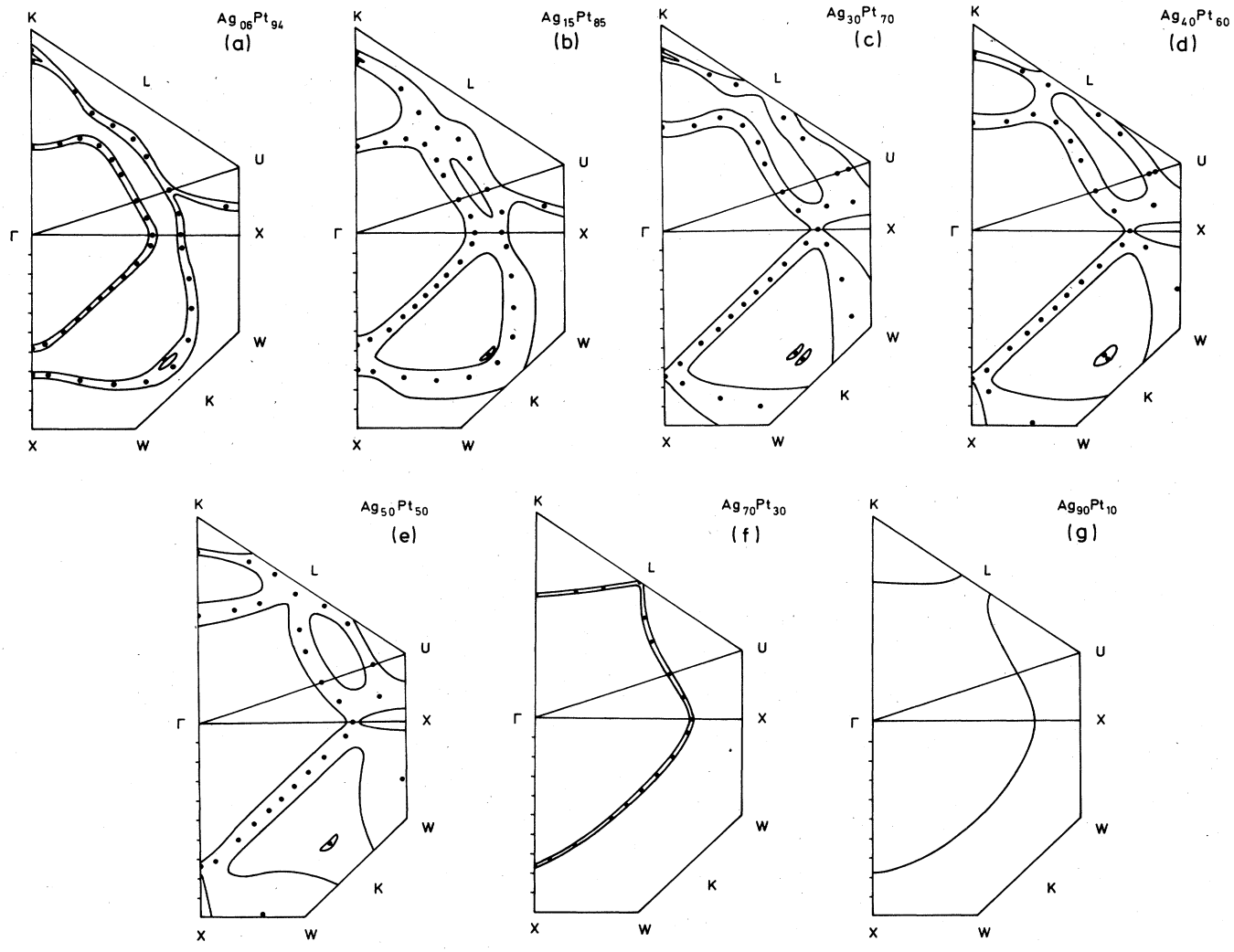

FIG. 8. Fermi surfaces for (a) Ag_6Pt_{94}, (b) $Ag_{15}Pt_{85}$, (c) $Ag_{30}Pt_{70}$, (d) $Ag_{40}Pt_{60}$, (e) $Ag_{50}Pt_{50}$, (f) $Ag_{70}Pt_{30}$, and (g) $Ag_{90}Pt_{10}$. In (a)—(f) the solid circles denote peaks in the Bloch spectral functions. The width of the Fermi-surface cuts shown corresponds to the half-width of the peaks in the Bloch spectral functions.

sp band at 2.65 and 1.6 eV, whereby the peak at 1.6 eV is considerably broader. For $Ag_{90}Pt_{10}$ there is still a peak at about 1.6 eV and a very distinguishable shoulder at about 2.5—3.0 eV.[14] Looking at Fig. 4(g) one can see two peaks in the contribution of Pt (dashed line) to the total density of states, namely at about 3 and 1.65 eV below the Fermi energy. In Fig. 6(g) the situation becomes even more clear. Here one can see two peaks in the Pt $d^{5/2}$—like partial local density of states at about 2.5 and 1.65 eV below the Fermi energy. The Pt $d^{3/2}$—like partial local density of states also shows a two-peak structure in this energy region, namely at about 3 and 2.5 eV. In the Bloch spectral function for $\mathbf{k}=(0,0,0)$, Fig. 9(f), the small peak to the right of the dominant Ag peaks is at about 2.5 eV below the Fermi energy. In particular, Fig. 6(g) suggests that in $Ag_{90}Pt_{10}$ the peak at 1.6 eV in the experimental spectrum arises from the corresponding peak in the $d^{5/2}$-like partial local density of states for Pt, while the shoulder at about 2.5—3.0 eV in the experimental spectrum is due to a superposition of the peak at 2.5 eV in the Pt $d^{5/2}$—like partial local density of states and the two peaks in the corresponding $d^{3/2}$-like density of states. For $Ag_{98}Pt_2$, van der Marel *et al.*[14] claim that the two-peak structure in the UPS is essentially due to the O_h double-group splitting of atomic Pt *d* levels. Their splitting between the Γ_8^+ ($d^{3/2}$) and Γ_8^+ ($d^{5/2}$) levels of about 1.2 eV seems to be reasonable, as compared to the atomic $d^{3/2}$-$d^{5/2}$ splitting of 1.43 eV. Their interpretation, however, seems to be in contrast to the interpretation given by Smith.[16] For $Ag_{90}Pt_{10}$ the partial local Pt *d*—like densities of states give a reasonably good account for the two-peak structure observed experimentally. Without a proper calculation of the photocurrent, however, an interpretation solely in terms of density-of-states functions must remain somewhat ambiguous.

Since the Ag-Pt system has a large miscibility gap,[10] a comparison of theoretical and experimental values can be rather difficult. Despite this difficulty, as already men-

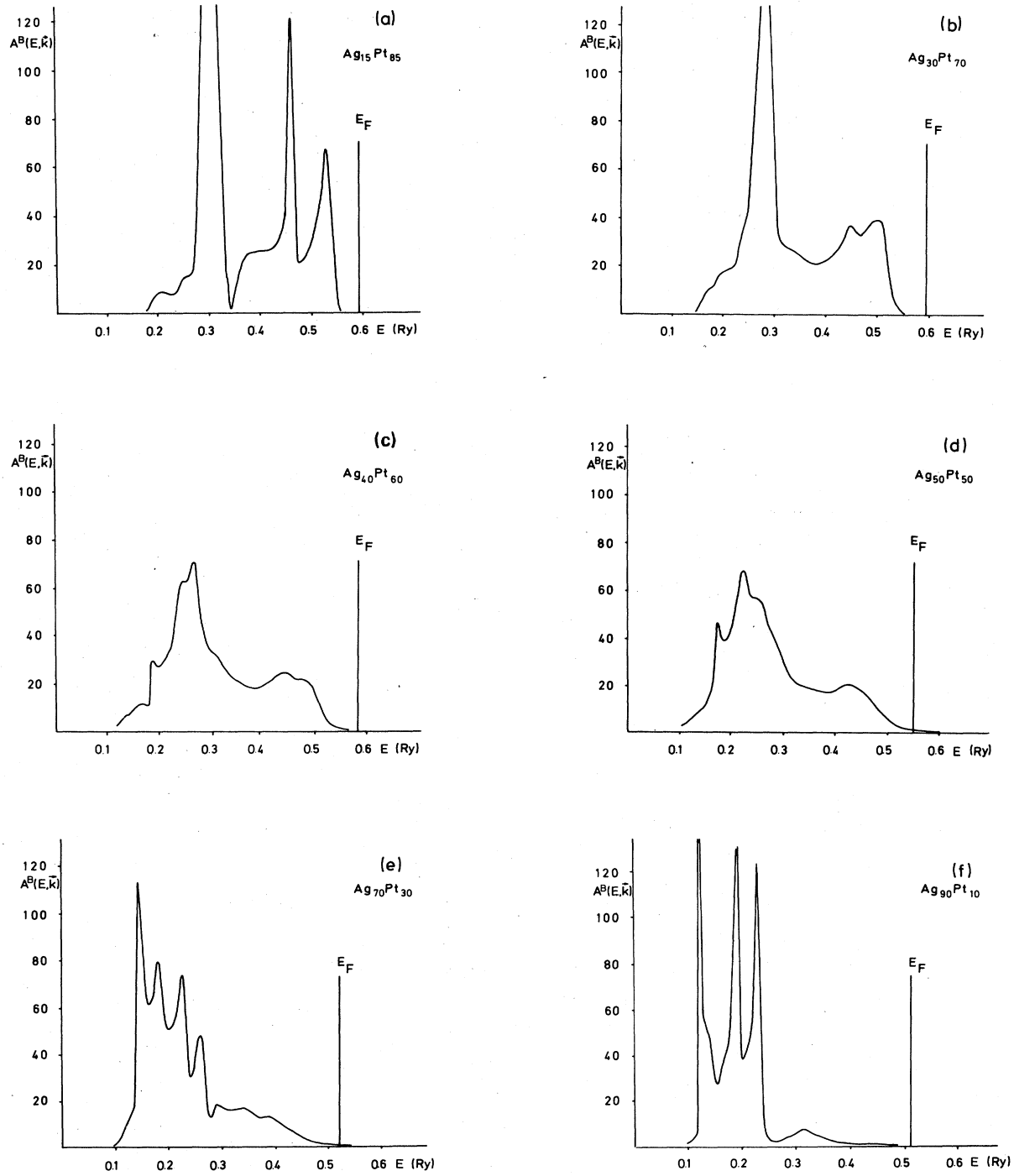

FIG. 9. Bloch spectral functions for $\mathbf{k}=(0,0,0)$ for (a) $Ag_{15}Pt_{85}$, (b) $Ag_{30}Pt_{70}$, (c) $Ag_{40}Pt_{60}$, (d) $Ag_{50}Pt_{50}$, (e) $Ag_{70}Pt_{30}$, and (f) $Ag_{90}Pt_{10}$.

tioned, the calculated values for the density of states at the Fermi energy fit the experimental molar susceptibilities rather well.[11] Using the present KKR-CPA results the calculated nuclear-spin-lattice relaxation rates for Ag and Pt are in reasonably good agreement[9] with the experimental rates.[11,17] The same kind of agreement was found for the system Ag_xPd_{1-x},[5,18] using the self-consistent (nonrelativistic) KKR-CPA method. The experimental NMR data seem to confirm the calculated spectral quantities (for a detailed discussion of the nuclear-spin-lattice relaxation rates, see Ref. 9).

It should be noted that quite a few physical properties can be extracted from the results shown in Figs. 4—8. The partial local densities of states, for example, are

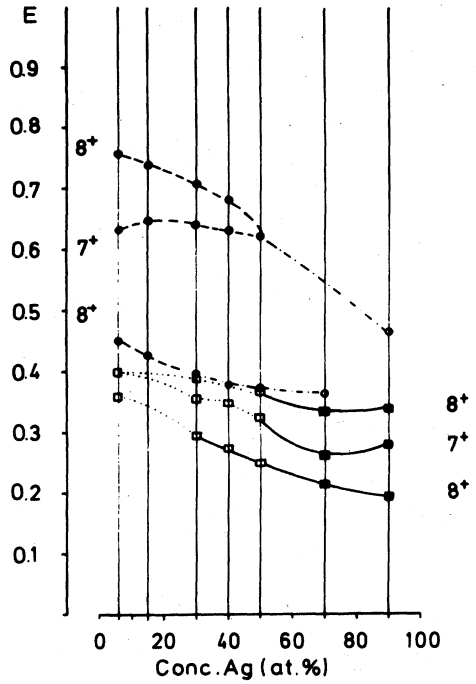

FIG. 10. Peak positions for the $\mathbf{k}=(0,0,0)$ Bloch spectral functions in Ag_xPt_{1-x}. Solid circles denote the energy position [energy in dimensionless units: 1 d.u.$=(a/2\pi)^2$ Ry] of sharp Pt-like peaks, open circles denotes that for weak Pt-like peaks, solid squares that for sharp Ag peaks, and open squares that for weak Ag-like peaks.

mapped in soft-x-ray—emission spectra for the components Ag and Pt; the Fermi surfaces can be measured experimentally using positron annihilation, etc.

V. CONCLUSION

The present calculations are non-self-consistent with respect to the scattering potentials. From Ref. 9 it seems that charge-transfer effects are not of crucial importance for the electronic structure in Ag_xPt_{1-x}. It also seems that, at least for $Ag_{90}Pt_{10}$, the density of states, particularly the partial local density of states for Pt, fit the observed "impurity" peaks in the UPS spectra rather well. It remains to be seen, however, whether, in a detailed angle-resolved photoemission experiment, the same kind of agreement with the theoretical results can be achieved when compared to a proper calculation for the angle-resolved photocurrent. At present, one must rely on the scattering potentials used, since self-consistent, fully relativistic KKR-CPA calculations are only feasible for very selected problems of general interest, such as, for example, the order-disorder transition in Cu_3Au,[19] where only one concentration has to be studied.

ACKNOWLEDGMENTS

One of us (H.E.) wishes to acknowledge a grant from the Deutscher Akademischer Austausch Dienst (DAAD). All calculations were performed using the facilities of the Technical University of Vienna Computing Centre.

[1]B. L. Gyorffy and G. M. Stocks, *Electrons in Disordered Metals and Metallic Surfaces* (NATO Advanced Study Institute Series B42), edited by P. Phariseau, B. L. Gyorffy, and L. Scheire (Plenum, New York, 1979), p. 89.
[2]J. S. Faulkner, Prog. Mater. Sci. **27**, 1 (1982).
[3]J. S. Faulkner and G. M. Stocks, Phys. Rev. B **21**, 3222 (1979).
[4]J. Staunton, B. L. Gyorffy, and P. Weinberger, J. Phys. F **10**, 2665 (1980).
[5]H. Winter and G. M. Stocks, Phys. Rev. B **27**, 882 (1983).
[6]P. Weinberger, J. Staunton, and B. L. Gyorffy, J. Phys. F **12**, 2229 (1982).
[7]H. Winter, P. J. Durham, G. M. Stocks, and W. M. Temmerman, Phys. Rev. B (to be published).
[8]J. Staunton, P. Weinberger, and B. L. Gyorffy, J. Phys. F **13**, 779 (1983).
[9]H. Ebert, P. Weinberger, and J. Voitländer, following paper, Phys. Rev. B **31**, 7566 (1985).
[10]H. Ebert, J. Abart, and J. Voitländer, J. Less-Common Met. **91**, 89 (1981).
[11]H. Ebert, J. Abart, and J. Voitländer, J. Phys. F **14**, 749 (1984).
[12]P. Weinberger, J. Phys. F **12**, 2171 (1982).
[13]H. Eckhardt, L. Fritsche, and J. Noffke, J. Phys. F **14**, 97 (1984).
[14]D. van der Marel, G. A. Sawatzky, and J. A. Julianus, J. Phys. F **14**, 281 (1984).
[15]S. Hufner, G. K. Wertheim, and J. H. Werwick, Solid State Commun. **17**, 1585 (1975).
[16]P. V. Smith, J. Phys. F **11**, 1063 (1981).
[17]H. Herberg and J. Voitländer, Phys. Rev. B **22**, 5043 (1980).
[18]H. Ebert, H. Winter, and J. Voitländer, J. Phys. F **14**, 2433 (1984).
[19]R. G. Jordan, G. S. Schal, B. L. Gyorffy, P. J. Durham, W. M. Temmerman, and P. Weinberger, J. Phys. F (to be published).